IOPscience iopscience.iop.org

Home Search Collections Journals About Contact us My IOPscience

Yield strength, shear stress and toughness of YBCO samples textured by Bridgman technique

This article has been downloaded from IOPscience. Please scroll down to see the full text article.

2008 J. Phys.: Conf. Ser. 97 012116

(http://iopscience.iop.org/1742-6596/97/1/012116)

View the table of contents for this issue, or go to the journal homepage for more

Download details:
IP Address: 147.83.132.21
The article was downloaded on 19/11/2012 at 09:09

Please note that terms and conditions apply.

Yield strength, Shear Stress and Toughness of YBCO samples textured by Bridgman technique

J J Roa[1], E Jiménez-Piqué[2], X G Capdevila[1], M Martínez[1], M Segarra[1]

1 Centro DIOPMA, Departamento de Ciencia de los Materiales e Ingeniería Metalúrgica; Instituto de Nanociencia y Nanotecnología de la Universidad de Barcelona (IN^{2}UB). Facultad de Química, Universidad de Barcelona, Martí i Franqués 1, Barcelona 08028, Spain.

2 Departamento de Ciencia de los Materiales y Ingeniería Metalúrgica. Universidad Politécnica de Cataluña, Diagonal 647 (ETSEIB), Barcelona 08028, Spain.

E-mail: joanjosep_roa@ub.edu

Abstract. Mechanical properties of the orthorhombic phase of $YBa_2Cu_3O_{7-\delta}$ (Y-123) at room temperature have been investigated at different applied loads using nanoindentation technique. The study was carried out for several monodomains on the (001) planes for textured Bridgman samples with dispersed Y_2BaCuO_5 (Y-211) particles as pinning centers. The yield strength (σ_{ys}), shear stress (τ_m) and toughness (K_{IC}) of Y123/Y211composite was determined at different applied loads. First and second mechanical properties have been calculated though the Hertz equations and the last one with Lawn et al. equations. Finally, the ultra-low imprints obtained by nanoindentation have been correlated with parameters obtained by Field Emission Scanning Electron Microscope (FE-SEM).

1. Introduction

It is well known that bulk superconductor materials exhibit high critical current density and high magnetic field at cryogenic temperatures (liquid nitrogen). In order to prepare bulk pieces, a fine and well-dispersed Y-211 precipitate distribution in the Y-123 matrix has to be achieved.

Most superconducting applications of interest for electric utilities require superconductors in the form of bulk, wire or tape. Useful superconductors need to be flexible, ductile and carry large current densities. Hence, the extreme brittleness of ceramics is the leading obstacle to the practical implementation of high temperature superconductors (HTSCs). It has been suggested that these poor mechanical properties limit the performance of melt-textured YBCO in applications where magnetic field and/or thermal cycling is unavoidable[1].

Nanoindentation is a versatile technique for measuring mechanical properties at very small scale, namely in the micron and sub-micron range [2]. Nanoindentation is a non-destructive and selective technique. It can work from 50 nN to 500 mN.

The purpose of this experimental study is to determine the yield strength, shear stress and fracture toughness of Y-123/Y-211$_{composite}$ at room temperature. So different loads (5, 10, 30 and 100 mN) have been applied on the ab plane (001) of textured Bridgman samples.

© 2008 IOP Publishing Ltd

Yield Strength, Shear Stress of Y-123/Y-211 composite have been calculated through Hertz equations and Toughness with Lawn et al. equations [3-4].

2. Experimental procedure

2.1. Preparation of bulk YBCO pieces and monodomain growth

The YBCO powders were prepared by PVA method [5]. Ratio used here (69% w/w Y123, 30% w/w Y211 and 1% w/w $CeO_2 \cdot nH_2O$) has been demonstrated to maximize critical current density [6]. The standard composition of the starting material was Y-123 with an Y-211 excess of 30% w/w. $CeO_2 \cdot nH_2O$ was added in order to achieve a refinement of the Y-211 distribution. The calcined powder was deagglomerated by ball milling in an agate mortar.

Green bulk pieces were obtained by uniaxial isostatic cold pressure and further textured using the Bridgman method [6-8]. After this, bulk textured pieces were oxygenated in a horizontal furnace at 450 ºC for 240 h [9]. From the oxygenated pieces with a common c-axis tilt of 45º, small pieces of 2 mm height were cut by the (001) planes[1].

2.2. Mechanical Properties

Nanoindentation test were performed with a Nano Indenter® XP system (MTS Systems Corporation) equipped with Test Works 4 Professional level software. Nanoindentation imprints were observed with field emission Hitachi H-4100 scanning electron microscope (SCT Barcelona). The experiments were performed on the (001) plane at room temperature. Applied loads were 5, 10, 30 and 100 mN. The loading/unloading time was selected to be constant for all indentations, 15 s.

The nanoindentations were made by a three-sided pyramid Berkovich diamond indenter. The displacement (*penetration depth*) was continuously monitored and load-time history of indentation recorded. The tip was calibrated with a fused silica standard and the frame stiffness and the thermal drift were automatically corrected.

2.2.1. Yield strength and Shear Stress

The yield strength of YBCO bulk was calculated from the nanoindentation hardness value using Hertz equations for blunt contact [3].

Figure 1 presents a scheme of load-penetration depth (P-h) curve for a sharp indenter with its associate nomenclature. During the first steps of indentation the curve follows the relation, $P = C \cdot h^{3/2}$. This relation corresponds to the elastic deformation, and the yield strength can be obtained with the Hertzian equations, where C is the indentation curvature, which is a measure of the "resistance" of the material to indentation. This is due to the fact that the tip is rounded and, therefore, follows the equations for elastic contact with a blunt indenter. When the applied load induces a plastic deformation of material during loading process, the curve generally follows the next relation, $P = C \cdot h^2$, typical of a sharp indenter. Yield strength is defined as the stress at which a material begins to plastically deform. Prior to yield point the material will deform elastically and will return to its original shape when the applied load is removed. Once the yield point is passed, some fraction of the deformation will be permanent and non-reversible.

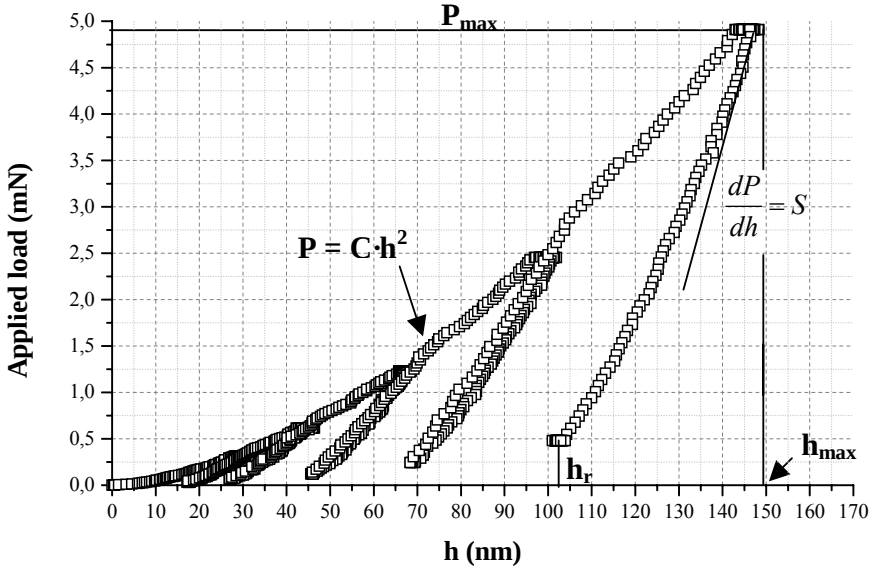

Figure 1. Loading/unloading curve when the applied load was 5 mN.

Hertz equations

The stresses and deflection arising from the contact between two elastic solids are of particular interest to those understand the first steps of indentation testing. The contact between a rigid sphere and a flat surface for small penetration depths was described by Hertz. This phenomena is shown in Figure 2 [3]. The radius of the circle of contact is a, the total depth of penetration is h_t, the depth of the circle of contact from the specimen free surface h_a, and h_p is the distance from the bottom of the contact to the contact circle.

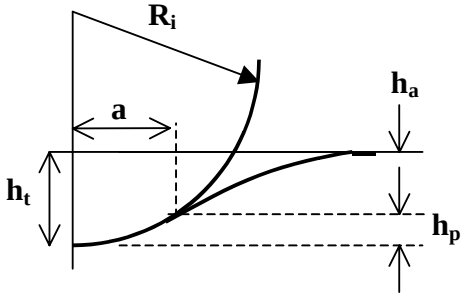

Figure 2. Scheme of the contact between a rigid indenter and a flat specimen at first steps of indentation (elastic contact).

Hertz [12] found that the radius of the circle of contact a, is related to the indenter load, P, the indenter radius, R, and the elastic properties for small penetration depths of the material by:

$$a^3 = \frac{3}{4} \cdot \frac{P \cdot R}{E_{eff}} \tag{1}$$

where E_{eff} is the effective modulus between the sample and the indenter. E_{eff} can be rewritten as:

$$\frac{1}{E_{eff}} = \frac{1-\nu^2}{E} + \frac{1-\nu_i^2}{E_i} \tag{2}$$

where E and ν are the Young's modulus and Poisson's ratio for material of study and E_i, ν_i are the Young's and Poisson's moduli for the indenter (E_i=1140GPa and ν_i=0.07 [11]), respectively.

The mean contact pressure, p_m, between the indenter and the material is:

$$p_m = \frac{P}{\pi \cdot a^2} = \frac{4 \cdot E_{eff}}{3 \cdot \pi} \cdot \left(\frac{a}{R} \right) \tag{3}$$

The mean contact pressure is often referred to as the "indentation stress" and the quantity a/R as the "indentation strain".

The maximum tensile stress occurs at the edge of the contact circle in the surface and can be calculated by [10]:

$$\sigma_{\max} = \frac{1}{2} \cdot (1 - 2 \cdot \nu) \cdot p_m \tag{4}$$

The maximum tensile stress is the yield strength of the material. This parameter will make the transition from elastic to elastic-plastic response [12].

The maximum shear stress (τ_m) is produced beneath the indentation axis at a depth close to 0.5·a, and equals to:

$$\tau_m = 0.46 \cdot p_m \tag{5}$$

The maximum shear stress, is also known as the Tresca criterion. This assumes that yield occurs when the shear stress τ exceeds the shear yield strength τ_{ys}:

$$\tau = \frac{\sigma_1 - \sigma_3}{2} \leq \tau_{ys} \tag{6}$$

where σ_1 and σ_3 are principal stress (also, can be rewritten as σ_x and σ_z, respectively).

2.2.2. Toughness

Conventional indentation toughness methods were initially developed for monolithic bulk materials tested by microindentation when well-developed radial cracks form [3]. The fracture toughness K_{IC} is related to the applied load, P, and the crack dimension, c.

When a external stress (residual stress "σ_r") is applied to the sample, the crack will assume a new equilibrium length, c. The stress intensity can be expressed as [4]:

$$K_{IC} = K_i + K_r = \chi \cdot \left(\frac{E}{H} \right)^{1/2} \cdot \frac{P}{c^{3/2}} + \psi \cdot \sigma_r \cdot c^{1/2} \tag{7}$$

where, K_i is the indentation stress intensity factor, K_r is the residual stress intensity factor, χ is a constant that is a function of the indenter (for a Berckovich indenter, χ = 0.016), E and H are the Young's Modulus and Hardness of the studied material, and ψ is a constant related to the crack geometry and loading conditions. If only one surface cracks are considered, then $\psi = \pi^{1/2}$ [13].

Normally, the residual stress intensity factor is lower than the indentation stress intensity factor. For this reason, equation 7 can be re-written as follow:

$$K_{IC} = \chi \cdot \left(\frac{E}{H} \right)^{1/2} \cdot \frac{P}{c^{3/2}} \tag{8}$$

3. Results and Discussion

Load/Unload curves, Nanohardness and Young's modulus values used to calculate yield strength, shear stress and toughness had been obtained in a previous work [14].

3.1. Yield strength and Shear Stress

The indenter radius, R, has been determine by FE-SEM, and the value is 460 nm. Figure 3, shows the calculated yield strength and shear stress values of the orthorhombic Y-123/Y-211 composite for the different monodomain samples studied when the applied loads were 5, 10, 30 and 100 mN. Each point in Figure 3 is an average of 40 measurements performed on two different samples in order to achieve statistical significance.

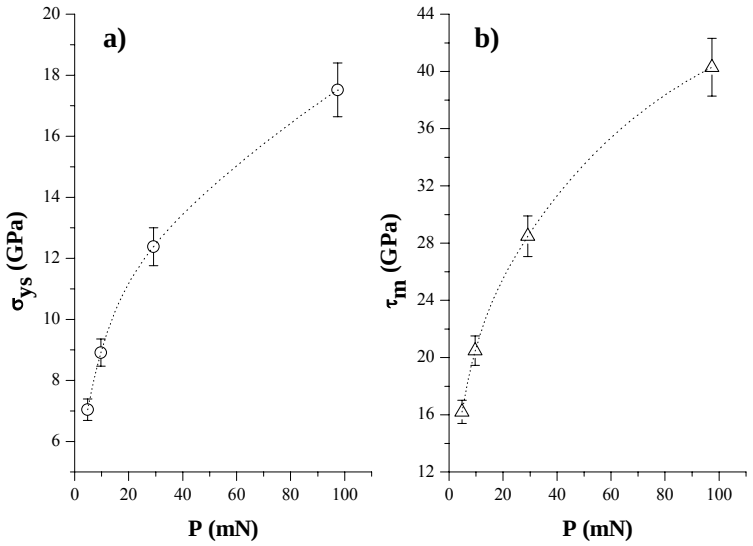

Figure 3. The relationship between a) yield strength and applied load and b) shear stress and applied load.

In Figure 3, it can be observed that yield strength and shear stress display a exponential law. Moreover, yield strength and shear stress can be strongly affected by the presence of defects and impurities, that can cause almost no change in dislocation movement, which would affect these mechanical properties. We can observe that both mechanical properties increase when the applied load is increased. It is due to surface defects. Yield strength of Y-123/Y-211 composite is lower than shear stress. This fact could be due to different reasons: (a) shear stress only depends on the mean contact pressure, p_m, and yield strength depends on p_m and also on the Poisson ratio (this is a intrinsic material property), and/or (b) the melt-processed ceramic composites contain a dense population of fine peritectic particles, acting as nucleation sites for dislocation onto a (001) plane, which affects drastically the microstructure [15] .

A relationship between yield strength and shear stress at different applied loads has been found (see Figure 3), which can be used to calculate yield strength and shear stress as a function of P. Therefore, from Figure 3 we obtain:

$$\sigma_{ys} = 4.25 + 5.67 \cdot \left(1 - e^{\left(-\frac{P}{9.09}\right)}\right) + 19.37 \cdot \left(1 - e^{\left(-\frac{P}{195.39}\right)}\right) \quad (9)$$

$$\tau_m = 8.83 + 28.35 \cdot \left(1 - e^{\left(-\frac{P}{65.04}\right)}\right) + 9.45 \cdot \left(1 - e^{\left(-\frac{P}{5.73}\right)}\right) \quad (10)$$

The integration of the first equation gives the work to perform a plastic deformation.

3.2. Toughness

In Figure 4, two types of indentations can be observed, one with a crack at the corners of the nanoindentation imprints performed at 30 mN, an the other one with porosity and radial cracks performed at 100 mN.

When the applied load is higher than 30 mN, the toughness can not be determined because the crack length can not be measured. In this case, other fracture factors exist, such as porosity due to the applied load or radial cracks (see Figure 4 b).

Toughness of this material can be only studied when applied load is 30 mN. When applied load is 10 mN or lower, the toughness value of each phase can not be calculated, because the length of the cracks at the Y-123 and Y-123/Y-211 composite imprints can not be observed. In spite of that, Y-211 present other fracture factors such as chipping [14].

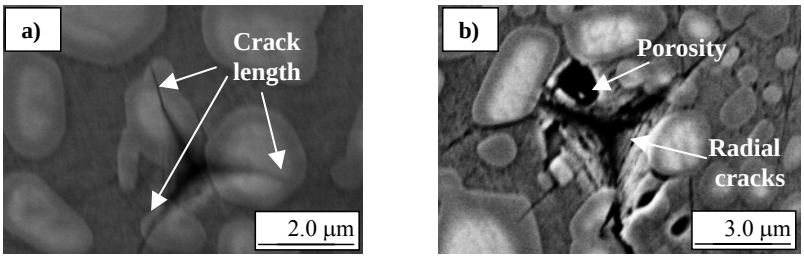

Figure 4. Nanoindentation imprints a) at 30 mN with crack propagation at the corners of the indentation, and b) at 100 mN with porosity and radial cracks.

With the crack length and the equation 8, the toughness can be calculated for an applied load of 30 mN. The obtained value is 2.85 ± 0.11 MPa·$m^{1/2}$.

4. Conclusions

Nanoindentation is a versatile and non-destructive technique to determine the mechanical properties of superconductor materials at ultra low load.

Yield strength and shear stress for Y-123/Y-211 composite by depend on exponential law with tha applied load. Therefore, these mechanical properties can be previously determined at a wide range of loads (from 5 to 100mN), with equations 9 and 10, respectively, with a 5% error.

If we integrate equation 9 between two different loads, we can calculate the minimum work necessary to perform a plastic deformation under this load range.

Fracture toughness can only be determined at 30 mN of applied load. The imprints obtained under higher loads present different fracture events such as: cracks only at one of the corners of nanoindentation imprint, porosity, chipping, etc.

5. Acknowledgments

The authors would like to thank Cermae (Generalitat de Catalunya) for financial support and Serveis Cientificotécnics for SEM.

References

[1] Ullrich M, Leenders A, Krelaus J, Kautschor L-O, Freyhardt H C, Schmidt L, Sandiumenge F and Obradors X 1998 *Mater. Sci. Engi.* B **53** pp. 143-148.
[2] Pharr G M 1998 *Mater. Sci. Eng. A* **253** pp.151.
[3] Fischer-Cripps A C 2004 Nanoindentation, Second Edition ISBN 0-387-22045-3.
[4] Soares P C and Lepienzki C M 2004 *Journal of Non-Crystalline Solids* **348** pp. 139-143.
[5] Serradilla IG, Calleja A, Capdevila XG, Segarra M, Mendoza E, Teva J, Granados X, Obradors X and Espiell F 2002 *Superconductor Science and Technology* **15** 566.
[6] Piñol S, Gomis V, Martín B, Labarta A, Fontcuberta J and Obradors X 1993 *Journal of Alloys and Compounds* **11** 195.
[7] Granados X, Piñol S, Martín B, Galante F, Sandiumenge F, Fontcuberta J and Obradors X 1994 *Cryogenics* **34** 833.
[8] Piñol S, Obradors X, Martín B, Fontcuberta J and Sandiumenge F. Patente ES-2111435.
[9] Mendoza E. *Tesis Doctoral,* Dept. de física aplicada, Universidad de Barcelona (2002).
[10] Fischer-Cripps A C 1999 *Journal of Materials Science* **34** pp. 129-137.
[11] Jiménez-Piqué E, Gaillard Y and Anglada M 2007 *Key Enginnering Materials* **333** 107-116.
[12] Giallard Y, Tomas C and Woirgard J 2003 *Phil. Mag. Let*. **9** pp. 553.
[13] Zeng K and Rowelife D J 1994 *Journal American Ceramics Society* **77** pp. 524.
[14] Roa J J, Capdevila X G, Martinez M, Espiell F and Segarra M 2007 *Nanotechnology* **18**, In Press.
[15] Sandiumenge F, Puig T, Rabier J, Plain J and Obradors X 2000 *Adv. Mater* **12** 375.